Article

Not peer-reviewed version

Tr-57 Treatment of SUM159 Cells Induces Mitochondrial Dysfunction without Affecting Membrane Potential

Artem Mishukov , Ekaterina Mndlyan , Alexey V. Berezhnov , Margarita Kobyakova , Yana Lomovskaya , Ekhson Holmuhamedov , Irina Odinokova *

Posted Date: 6 December 2023

doi: 10.20944/preprints202312.0356.v1

Keywords: TR-57; SUM159 TNBC cells; respiratory complexes: mitochondrial membrane potential; FoF1-ATPase; IF1; calcium-regulated mitochondrial ATP-Mg/Pi carrier

Article

TR-57 Treatment of SUM159 Cells Induces Mitochondrial Dysfunction without Affecting Membrane Potential

Artem Mishukov [1], Ekaterina Mndlyan [2], Alexey V. Berezhnov [3], Margarita Kobyakova [2], Yana Lomovskaya [2], Ekhson Holmuhamedov [2,*] and Irina Odinokova [2,*]

[1] Center of Theoretical Problems of Physico-Chemical Pharmacology, Russian Academy of Sciences;, Moscow, Russian Federation, 109029; artem.mishukov1999@gmail.com (A.M.)
[2] Institute of Theoretical and Experimental Biophysics, Russian Academy of Sciences, Pushchino, Moscow region 142290, Russian Federation; mndlyaneyu@gmail.com (E.M.); ritaaaaa49@gmail.com (M.K.); yannalomovskaya@gmail.com (Y.L.); ekhson@gmail.com (E.H.); odinokova@rambler.ru (I.O.)
[3] Institute of Cell Biophysics, Russian Academy of Sciences, Federal Research Center "Pushchino Scientific Center for Biological Research of the Russian Academy of Sciences", 142290 Pushchino, Moscow region Russian Federation; alexbereg56@gmail.com
* Correspondence: odinokova@rambler.ru (I.O.); ekhson@gmail.com (E.H.)

Abstract: Recent works identified ClpXP, mitochondrial caseinolytic protease, as the only target of imipridones - new class of antitumor agents. Our study of the mechanism of imipridone derivative TR-57 action in SUM159 human breast cancer cells demonstrated mitochondrial fragmentation, degradation of mitochondrial mtDNA and mitochondrial dysfunction, due to inhibition of Complex I and Complex II activity. Complete inhibition of oxidative phosphorylation accompanied with 90, 94, 88 and 87% decrease in the content of Complex I, II, III and IV proteins, respectively. The content of the F_OF_1-ATPase subunits decreased sharply by approximately 35% after 24 hours and remained unchanged up to 72 hours of incubation with TR-57. At the same time, a disappearance of the ATPIF1, natural inhibitor of mitochondrial F_OF_1-ATPase observed after 24 h exposure to TR-57. ATPase inhibitor oligomycin had no effect on the mitochondrial membrane potential in intact SUM159, whereas it caused a 65% decrease in TR-57-treated cells. SUM159 cells incubated with TR57 up to 72 hours retained the level of proteins facilitating the ATP transfer across the mitochondrial membranes: VDAC1 expression was not affected, while expression of ANT-1/2 and APC2 increased by 20% and 40%, respectively. Thus, our results suggest that although TR-57 treatment lead to complete inhibition of respiratory chain activity of SUM159 cells, hydrolysis of cytoplasmic ATP by reversal activity of F_OF_1-ATPase supports mitochondrial polarization.

Keywords: TR-57; SUM159 TNBC cells; respiratory complexes: mitochondrial membrane potential; F_OF_1-ATPase; IF1; calcium-regulated mitochondrial ATP-Mg/Pi carrier

1. Introduction

Recently, a new class of imipridone-derived antitumor molecules including maternal TRAIL-inducing compound ONC201/TIC10 [1] and newly synthetized derivatives known as TR-compounds (Madera Therapeutics, Chapel Hill, NC USA) [2] attracted the attention of investigators. The first data set on the potent efficacy of the first-in-class small molecule ONC201 were published in 2013 [3] and over 10 years, a lot of preclinical work has appeared on tumor cells related to hematological and solid malignancies including prostate, breast, ovarian lung, pancreatic cancer cell lines as well as leukemia, lymphoma, glioma and hepatocellular cancer cells [4]. The broad specificity of the action of imipridones, high efficiency, and selectivity for tumor cells made it possible to use them in clinical trials [4–6]. While the early studies showed that the effect of imipridones on tumor cells occurs through inducing the expression of TRAIL and its receptor DR5 [3,7], as well as increasing the sensitivity of cells to exogenous TRAIL [8], recent observations demonstrated mitochondrial caseinolytic serine protease ClpXP, localized within the mitochondrial matrix as the only intracellular

 doi:10.20944/preprints202312.0356.v1

target for imipridones [2,9,10]. ClpP in the mitochondrial matrix forms a complex with the ATP-dependent protein unfoldase ClpX, which belongs to the AAA+ class (ATPase Associated with various cellular Activities) proteases [11]. The ClpXP complex is involved in mitochondrial quality control; its substrates are many mitochondrial proteins including proteins of electron transport chain (ETC), tricarboxylic acid (TCA) cycle, mitochondrial gene transcription and translation and ribosomal proteins [12]. Discovery of imipridones-induced activation of ClpP refocused investigators to study massive remodeling and unregulated proteolysis of proteins in mitochondria, accompanied with dramatic morphological changes and fragmentation of mitochondria, degradation of mitochondrial DNA and a rapid decrease in the level of mitochondrial transcription factor TFAM, responsible for maintaining the number of mtDNA copies [2,9,13–15]. In addition, RNA-sequencing of MB231 cells treated with ONC201 showed changes in the expression of genes responsible for maintenance of the mitochondrial genome and other mitochondrial processes, including oxidative phosphorylation [13]. In current work, we focused on the mechanism of action of TR-57 (chemically modified derivative of ONC201) with higher (50-100 times) efficacy compared to ONC201 [2,16,17], which is associated with a higher affinity of their binding to ClpP [2]. Multiple in vitro tests have shown that the antiproliferative effect of TR-57 is rather cytostatic and inhibits cell proliferation without induction of apoptotic cell death [13,18–20] and its cytostatic effect manifested not only by inhibition of tumor cells proliferation in vitro [2,21,22]. Characteristically, most of the studied breast cancer cell lines are characterized by the absence of induction of apoptosis under the influence of ONC201 or TR-57, only blocking of cell growth is observed [6], and with prolonged incubation with imipridones, the cells transform into a senescence-like phenotype [21,23]. However, it is still not completely clear what factors determine the sensitivity of cells to the action of imipridones, and the question of how imipridones-treated tumor cells containing mitochondria with impaired respiratory function maintain their viability remains unexplored.

Here we demonstrated that the mitochondrial component of the antiproliferative effect of TR-57 in cultured SUM159 human breast cancer cells consists of degradation the key structural and functional proteins of mtDNA translation and transcription, associated with decline in the expression of the key proteins of the respiratory Complexes I-IV, leading to suppression of the mitochondrial respiratory chain activity. Surprisingly, loss of the activity of mitochondrial respiratory chain was not associated with depolarization of remodeled mitochondria, and regardless of fragmentation and inhibition of electron transport, drug-treated cells retained mitochondrial membrane potential. Our data indicate that mitochondrial polarization could be supported by reversal of the activity of mitochondrial FoF1-ATPase, which, due to the consumption of glycolytic ATP, maintains the mitochondrial membrane potential necessary to perform mitochondrial functions and sustain the viability of tumor cells.

2. Results

2.1. Effect of TR-57 on mitochondrial morphology and the expression of key mitochondrial regulatory proteins in cultured SUM159 cells

In order to study the effect of TR-57 on the morphological and functional characteristics of mitochondria in human triple negative breast cancer cells SUM159, cells were exposed to 150 nM TR-57 for 24, 48 and 72 hours and stained with fluorescent dyes specific to mitochondria (Mito Tracker Deep Red 633 (MTDR)) and DNA (SYBR Green I). Figure 1a shows confocal fluorescent microscopy data, where mitochondria/mitochondrial mass are colored red (MTDR), double stranded mtDNA is colored green (SYBR Green-I), and cell nuclei are colored blue (Hoechst 33342). The data obtained on the confocal microscope were processed using ImageJ software [24] and the quantitative results are presented in Figure 1b–d. Incubation of SUM159 cells with TR-57 for 24 hours causes a decrease in the content of mitochondrial nucleoids from 91.06 ± 16.97 to 65.04 ± 4.85 nucleoids per cell; further incubation for 48 hours and 72 hours reduced the number of nucleoids to 53.93 ± 8.80 and 28.01 ± 2.97, respectively (Figure 1c). Decreased number of mtDNA after TR-57 treatment coincided with the decline in the content of TFAM and TUFM, key proteins involved in regulation of the stability,

Preprints (www.preprints.org) | NOT PEER-REVIEWED | Posted: 6 December 2023 doi:10.20944/preprints202312.0356.v1

transcription and translation of mtDNA, confirmed by Western blot analysis (Figure 1f). The content of mitochondrial elongation factor TUFM decreased to undetectable values after 24 hours of incubation with TR-57, while the level of mtDNA transcription factor TFAM decreases gradually with duration of the treatment and found in trace amounts after 72 hours (Figure 1f).

The average size of mitochondria stained with MTDR, which was calculated from confocal images, decreased approximately 2-fold after 24-hour incubation of cells with TR-57 and did not change significantly with further treatment (Figure 1c). MitoTracker Deep Red fluorescence intensity per cell, reflecting mitochondrial mass, decreased by 25% after 24 hours of incubation with TR-57, and with further incubation increased by 25%, however, the spread of values for different cells was quite large and the changes did not meet the reliability criterion (Figure 1d). Total mitochondrial content was also measured using flow cytometry, which showed that the average fluorescence intensity of MitoTracker Deep Red decreased by 40% over 24 hours and remained at this level until 72 hours of incubation with TR-57 (Figure 1e).

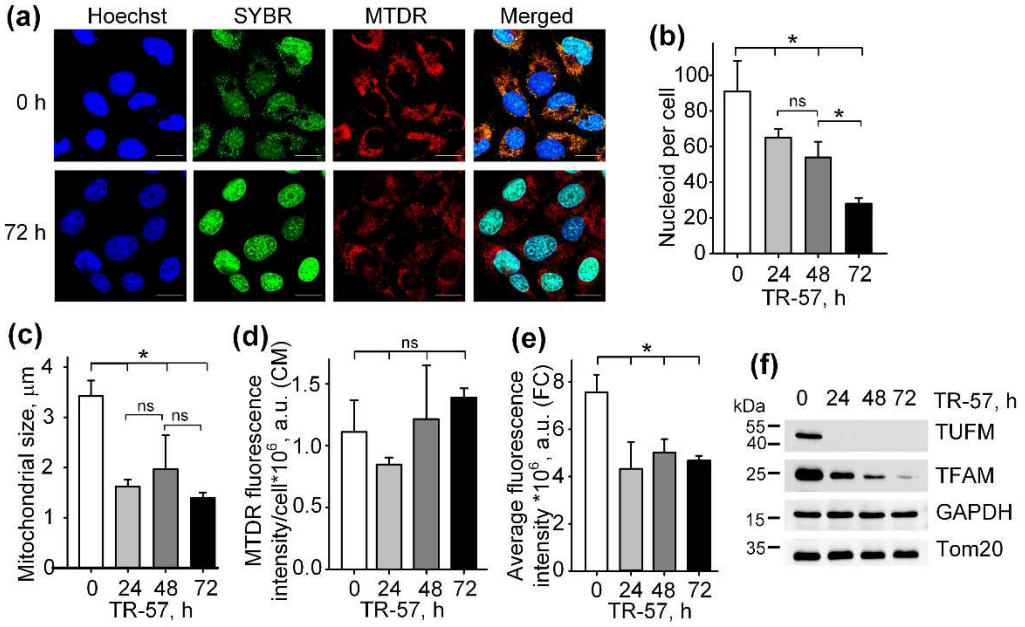

Figure 1. Effect of TR-57 on the number of mitochondrial nucleoids, mitochondrial morphology and size and the expression of key mitochondrial regulatory proteins of SUM159 cells. **(a)** representative confocal fluorescent images of intact (0 h) and treated with 150 nM TR-57 for 72 hours (72 h) SUM159 cells and loaded with Hoechst 33342 (Hoechst, blue), SYBR Green I (SYBR, green) and MitoTracker Deep Red (MTDR, red); Scale bar – 20 µm. Number of mitochondrial nucleoids **(b)**, average mitochondrial size **(c)** and average intensity of MitoTracker Deep Red fluorescence **(d)** in SUM159 cells treated with 150 nM TR-57 for 0 (intact), 24, 48 and 72 hours measured by confocal fluorescent microscopy (CM); **(e)** average intensity of MTDR fluorescence measured by flow cytometry (FC); **(f)** Western-blot analysis of mitochondrial proteins TUFM, TFAM and Tom20 in SUM159 cells treated with 150 nM TR-57 for 0, 24, 48 and 72 hours. The data are presented as the means ± SD of at least three independent experiments. The data were analyzed using a one-way ANOVA with post-hoc Bonferroni test. * – $p < 0.05$, ns – $p > 0.05$.

Thus, we confirmed previously published data that treatment of breast cancer cells with substances of the imipridone group (ONC201 and/or TR-57) causes a decrease in the content of mitochondrial nucleoids and mitochondrial fragmentation [13,21,25]. We have shown that the decrease in the number of nucleoids occurs gradually and depends on the time of incubation of cells with the agent, while the decrease in the size and number of mitochondria occurs in the first 24 hours and is not dramatic.

 doi:10.20944/preprints202312.0356.v1

2.2. Functional state of the respiratory chain of mitochondria in SUM159 cells treated with TR-57

In order to characterize the functional state of mitochondria in SUM159 cells treated with TR-57, we assessed mitochondrial oxygen consumption in a model of permeabilized cells in the presence of respiration substrates for Complex I (pyruvate + malate) and Complex II (rotenone + succinate) of the respiratory chain. Figure 2a shows typical recordings from an oxygen electrode, characteristic of cellular respiration using respiration substrates of the Complex I (Figure 2a). The tracing of oxygen concentration changes within the suspension after 0, 24, 48 and 72 hours of treatment of SUM159 cells with TR-57 (150 nM) shown in Figure 2a. First addition of 0.003% digitonin to the cell suspension and permeabilization of the plasma membrane (dig) lead to activation of the basal rate of respiration. The addition of 2 mM ADP (ADP) initiated a State 3 respiration (oxidative phosphorylation rate), which was blocked by the addition of 1 μM carboxyatractyloside (CATR), an adenine nucleotide translocator inhibitor (Figure 2a). The maximal (uncoupled) rate of respiration was achieved in the presence of 30 μM 2,4-dinitrophenol (DNP), and non-mitochondrial oxygen consumption was assessed in the presence of the cytochrome oxidase inhibitor NaN_3 (Figure 2a, NaN_3). Figure 2b demonstrates the averaged values of respiration rates using Complex I substrates for each time-points. These data demonstrate that 24 hours of incubation of cells with TR-57 suppresses oxidative phosphorylation (2.72±0.36 ng-atom O/min/10^6 cells in the control to 0.81±0.16 ng-atom O/min/10^6 cells) as well as uncoupled respiration (Figure 2B, ADP). Longer incubation of cells with TR-57 decreases oxygen consumption rate to 0.58±0.20 ng-atom O/min/10^6 cells. DNP-induced respiration rate decreases gradually from 2.29±0.18 ng-atom O/min/10^6 cells in the control to 1.14±0.06 ng-atom O/min/ 10^6 cells (24 hours with TR-57), 0.87±0.16 ng-atom O/min/10^6 cells after 48 hours and 0.54±0.05 ng-atom O/min/10^6 cells after 72 hours of incubation of cells with TR-57 (Figure 2b). Similarly, the respiration of SUM159 cells, oxidizing Complex II substrate, are affected by different duration of exposure to TR-57 as shown in Figure 2c,d,the typical recordings and the averaged values of the rate of respiration by digitonin-permeabilized SUM159 cells, oxidizing Complex II substrates, respectively. Thus, the both ADP-dependent and DNP-dependent respiration under these conditions reveal gradual decrease in respiration rates depending on the time of incubation of cells with the agent. State 3 (phosphorylating), respiration decreased from 3.82±0.53 ng-atom O/min/10^6 cells in the control to 2.04±0.38 ng-atom O/min/10^6 cells (24 hours of treatment), 1.30±0.25 ng-atom O/min/10^6 cells after 48 hours , and to 0.82±0.15 (72 hours of incubation) with TR-57. Similarly, an uncoupled respiration decreased from 3.05±0.65 ng-atom O/min/10^6 cells to 2.93±0.85, 1.72±0.49 and 0.92±0.22 ng-atom O/min /10^6 cells after 24, 48 and 72 hours, respectively. Thus, long-term incubation of SUM159 with 150 nM TR-57 result in consistent suppression of mitochondrial respiration supported by both, Complex I and Complex II substrates.

Observed inhibition of the respiratory activity of mitochondria following long-term exposure to TR-57 complemented by decline in the expression of the key proteins – subunits of the respiratory chain complexes of mitochondria, as demonstrated using Western blot analysis of specific proteins (Figure 2e–f: NDUFB8, subunit of Complex I; SDHD, subunits of Complex II; UQCRC2, subunit of Complex III; MTCO1, Complex IV subunit; ATP5A, subunit α of F_OF_1-ATPase, Complex V. We demonstrate that in SUM159 cells treated with 150 nM of TR-57 for 24 and 48 hours, the expression of subunits of Complexes I-IV decreases gradually as shown in Figure 2e,f. On average expression of NDUFB8 decreased by 48% and 86%, SDHD by 65% and 90%, subunit III UQCRC2 complex by 55% and 77%, respectively. The content of the mitochondrial-encoded subunit of complex IV decreased by 76% already in the first 24 hours of incubation with TR-57. Incubation of SUM159 with TR-57 for 72-hour and longer resulted in comparable decline in the expression of majority of these proteins to ~ 10% of the initial level of expression (untreated cells), except for ATP5A, Complex V, mitochondrial ATPase α subunit which decreased by 40% only in the first 24 hours exposure to TR-57 (Figure 2f).

Preprints (www.preprints.org) | NOT PEER-REVIEWED | Posted: 6 December 2023 doi:10.20944/preprints202312.0356.v1

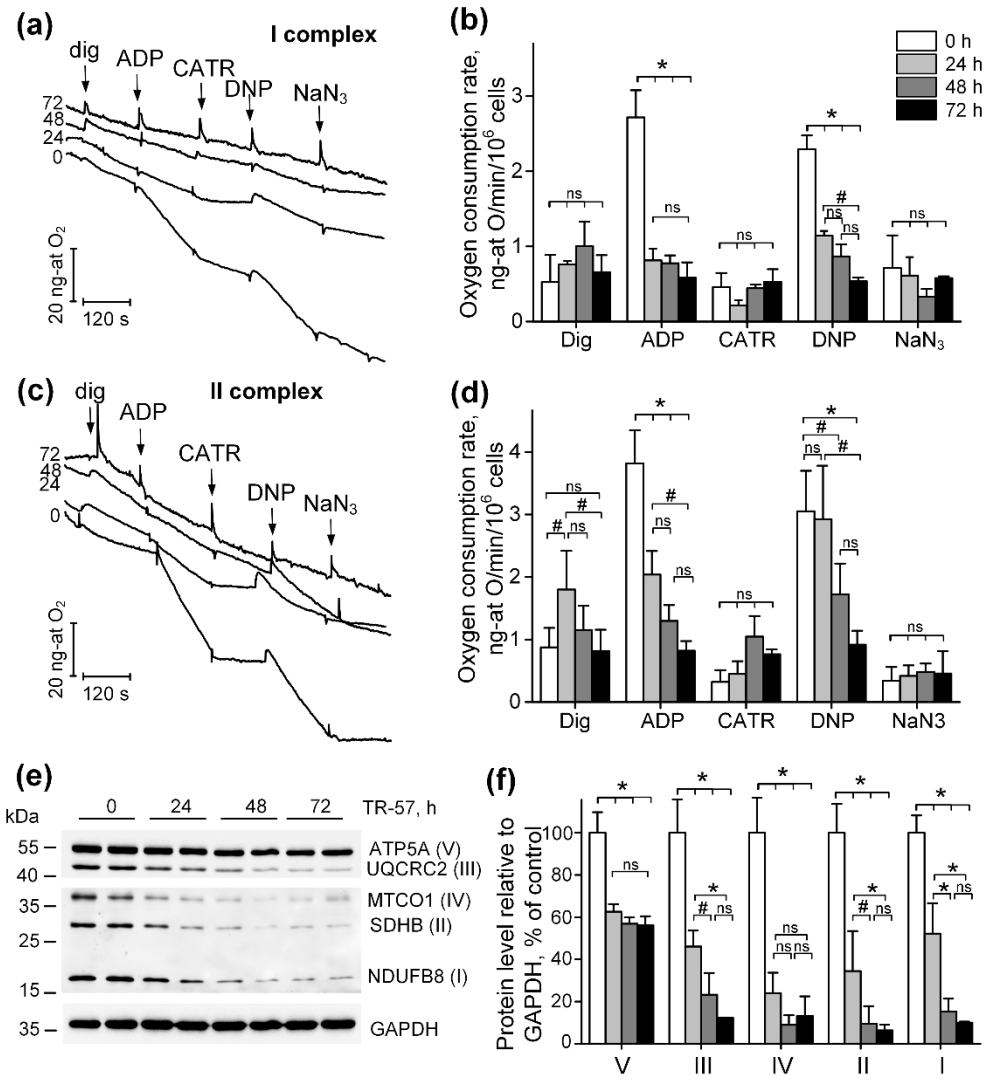

Figure 2. TR-57 induces gradual decrease in mitochondrial respiratory chain activity and electron transport chain (ETC) proteins content. **(a-b)** representative curves and oxygen consumption rates SUM159 cells, control (white bars) and treated with 150 nM TR-57 for 24 h (light gray bars), 48 h (dark gray bars) and 72 h (black bars), oxidizing Complex I substrates; **(c-d)** representative curves and oxygen consumption rates of SUM159 cells oxidizing Complex II substrates; Arrows on curves indicate additions of 0.003% digitonin, 2 mM ADP, 5 μM carboxyatractyloside (CATR), 30 μM 2,4-dinitrophenol (DNP) and 1 mM NaN3; **(e)** representative Western blot of ETC complex proteins; **(f)** quantitative analysis of ETC proteins normalized to GAPDH level. The ratio of protein level to GAPDH under control conditions was taken as 100%. The data are presented as the means ± SD of at least three independent experiments. The data were analyzed using a one-way ANOVA with post-hoc Bonferroni test. *p > 0.001, # p > 0.01, "ns" – non significant.

2.3. Effect of TR-57 on mitochondrial membrane potential

The mitochondrial membrane potential is the major component of the electrochemical gradient of hydrogen across the inner mitochondrial membrane generated by intact respiratory chain [5]. Despite the complete inhibition of the respiratory chain activity and induction of mitochondrial fragmentation, exposure of cultured SUM159 cells to TR-57 accompanied with minor mitochondrial depolarization (Figure 3). Mitochondrial membrane potential in cultured SUM159 cells assessed using two different potential-sensitive fluorescent dyes TMRM and DiOC6 (3) shown in Figure 3a,b and Figure 3c,d, respectively. Confocal images demonstrate that TMRM fluorescence decreased, but the calculated fluorescence intensity per pixel, which actually reflects the level of potential in

 doi:10.20944/preprints202312.0356.v1

individual mitochondria, remained unchanged in the first 48 hours of incubation and reduced by approximately 40% after 72 hours of incubation (Figure 3a,b). Similarly, using DiOC6 (3) and flow cytometry of SUM159 cells we demonstrated retention of 70% of mitochondrial polarization in these cells after 24, 48 and 72 hours of exposure to TR-57 (Figure 3c,d).

Typical confocal images of SUM159 cells with TMRM-stained mitochondria subjected to sequential treatment with Oligomycin (inhibitor of F_OF_1-ATPase), Antimycin A (inhibitor of respiratory chain) and CCCP (protonophoric uncoupler of oxidative phosphorylation) demonstrate the level of depolarization of mitochondria after each specific inhibitor in intact and TR-57 treated cells (Figure 3e). Quantification of the intensity of TMRM in intact SUM159 using described protocols demonstrated time dependent changes in the fluorescence of TMRM induced with Oligomycin, Antimycin A and CCCP (Figure 3f). In control cells, Oligomycin did not cause a noticeable decrease in TMRM fluorescence, and, consequently, the potential, while the addition of Antimycin A led to a drop in potential by 80% and the residual membrane potential was depolarized in the presence of CCCP (Figure 3b). Application of the same protocol of inhibitors to TR-57 treated SUM159 cells allowed to monitor the effect of TR-57 exposure on the source of TR-57-insensitive membrane potential. The cells incubated with TR-57 for 24 hours demonstrated that the sensitivity of TMRM fluorescence to inhibitors similar to that in Control cells (compare Figure 3b, 0 h and 24 h). In contrast, in cells treated with TR-57 for 72 hours, demonstrated 65% decrease in the intensity of TMRM fluorescence after inhibition of F_OF_1-ATPase with Oligomycin, and addition of Antimycin A caused the drop of the fluorescence to almost zero level and the uncoupler had no further effect (Figure 3b, 72 h). In contrast, in cells treated with TR-57 for 72 hours, there was a 65% decrease in potential after inhibition of F_OF_1-ATPase with Oligomycin; addition of antimycin A caused the potential drop to almost zero level and the uncoupler had no further effect.

Thus, we have shown that in control cells and cells treated for 24 hours with TR-57, the mitochondrial membrane potential supported through the work of the respiratory chain, while mitochondrial F_OF_1-ATPase generates longer treatment with TR-57 for 72 hours, the potential mainly due to ATP hydrolysis.

Mitochondria are capable of generating inner membrane potential not only through respiration but also through the hydrolysis of ATP to ADP by mitochondrial ATPase in reverse mode [26]. In this regard, we studied if TR-57 exposure affects the intactness and composition of proteins of F_OF_1-ATPase. As shown in Figure 2e–f, the content of subunit α of F_OF_1-ATP synthase in SUM159 cells decreased by 40% within first 24 hours of incubation with TR-57 and remained unchanged with prolonged (72 hours) treatment. TR-57 also induced similar decline in expression of the β protein of F_1 catalytic subunit of ATP synthase, located in the matrix, decreased by 25% after 24 hours of incubation and by 40% after 48-72 hours of incubation (Figure 3g–h). The level of the subunit b of membrane portion F_O of ATP synthase decreased by 30-40% within 24 hours and remains at this level until 72 hours of incubation of cells with TR-57. The level of another subunit of the F_O, subunit c, which forms the c-ring channel in the inner membrane, through which the H+ ion is transported during ATP synthesis, drops by 20% in the first 24 hours of treatment of TR-57 cells, and then even increased by 20% compared to control cells. This increase in protein level may be due to accumulation of the subunit c in the cell, which occurs under certain pathological conditions and may be a consequence of both its reduced degradation [27] and increased expression [28]. However, treatment of SUM159 cells with the TR57 component resulted in a complete disappearance of IF1, a natural inhibitor of the hydrolysis activity of ATP synthase (Figure 3g–f). Thus, the preservation of a sufficient number of copies of ATPase and the absence of the hydrolysis inhibitory factor IF1 allows us to say that when treated with TR-57, mitochondria of SUM159 cells can maintain the membrane potential due to the reversal of FoF1-ATPase.

Preprints (www.preprints.org) | NOT PEER-REVIEWED | Posted: 6 December 2023 doi:10.20944/preprints202312.0356.v1

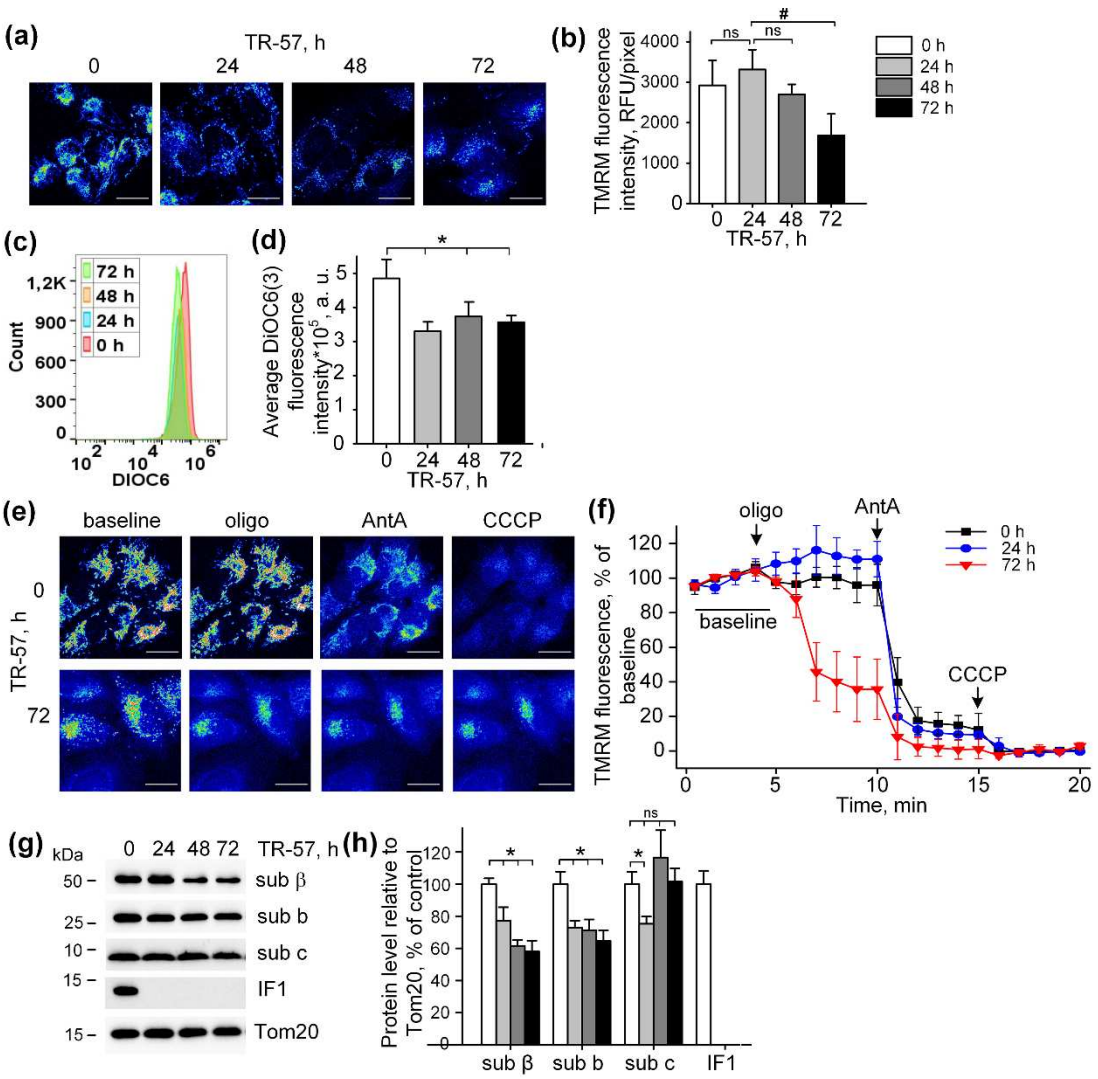

Figure 3. Effect of TR-57 treatment on mitochondrial membrane potential of SUM159 cells. (a) Representative confocal fluorescent images of SUM159 cells treated with 150 nM TR-57 for 0 (control), 24, 48 and 72 hours and stained with 20 nM TMRM; **(b)** Average intensity of TMRM in mitochondria of SUM159 from panel **(a)**; **(c-d)** Mitochondrial membrane potential of control (0) and TR-59 treated SUM159 cells measured with DiOC3(6) fluorescent dye by flow cytometry; **(e)** Representative confocal fluorescent images of SUM159 cells treated with 150 nM TR-57 for 0 (control) and 72 hours, stained with 20 nM TMRM and sequentially exposed to 2 μM Oligomycin (Oligo), 5 μM Antimycin A (AntA) and 1 μM CCCP; **(f)** Relative mitochondrial membrane potential of SUM159 from panel E during sequential addition of Oligo, AntA and CCCP, fluorescence of TMRM was normalized to 100% baseline and 0% after CCCP addition. **(g-h)** Representative Western blots and quantitative analysis of F_OF_1-ATPase proteins of SUM159 cells following treatment with 150 nM TR-57 for 0 (white bars), 24 h (light gray bars), 48 h (dark gray bars) and 72 h (black bars). Tom20 was used as loading control. The ratio of protein level to Tom20 under control conditions was taken as 100%. Scale bar is 20 μm. The data are presented as the means ± SD of at least three independent experiments. The data were analyzed using a one-way ANOVA with post-hoc Bonferroni test. *p > 0.001, # p > 0.01, "ns" – non significant.

2.4. Effect of TR-57 on the content of mitochondrial transport proteins

It was previously shown that imipridones (ONC201 and/or TR-57) induce the switch of metabolism from oxidative-phosphorylating to glycolytic in many cell cultures [13–15,17,29,30], including SUM159 cells. Our observation that mitochondrial dysfunction induced by TR57 was associated with partial depolarization of mitochondria indicate that mitochondrial membrane

Preprints (www.preprints.org) | NOT PEER-REVIEWED | Posted: 6 December 2023 doi:10.20944/preprints202312.0356.v1

potential in TR57 treated cells is maintained through reversal of mitochondrial F_OF_1-ATPase and utilization of the cytosolic ATP, transported into the matrix via transporters. We examined the content of some proteins that may be involved in ATP transport into mitochondria and the dynamics of their changes when cells were treated with TR-57. Figure 4a,b shows that the level of voltage-dependent anion channel protein (VDAC1), which transports ATP as well as other nucleotides and ions across the outer mitochondrial membrane, did not change during incubation with TR-57 up to 72 hours, and even a slight (non-significant) increase in its content is observed. The level of the proteins ATP/ADP transporters ANT1 and ANT2, responsible for the voltage-dependent exchange of ATP for ADP through the inner mitochondrial membrane, increased by 20% (ANT1) or did not change (ANT2) at 24 hours of incubation with TR-57. After 48 hours it is observed an increase in protein level by 60% and 30%, respectively; by 72 hours of treatment with TR-57, the content of ANT1/2 slightly decreased, but still remains 20% higher than in control cells. Mitochondria also contain the channels that can transport ATP into the matrix in exchange for inorganic phosphate (Pi) – the so-called calcium-regulated mitochondrial ATP-Mg/Pi carriers (APCs or SCaMCs). As shown in Figure 4a,b, the abundance of APC1 (SCaMC-1, SLC25A24) reduced by 40% after 24 hours and this protein almost completely disappeared after 48 hours of incubation with TR-57. However, the expression of another isoform APC2 (SCaMC-3, SLC25A23) increased by 40% in the first 24 hours and doubled after 48 hours of incubation. In addition, an increase in the content of inorganic phosphate transport protein (PiC, SLC25A3) is observed up to 40% after 72 hours of incubation with drug. Thus, we can say that ATP transport into the mitochondrial matrix of TR-57-treated cells for subsequent hydrolysis occurs through ANT1/ANT2, or, more likely, with the participation of APC-2.

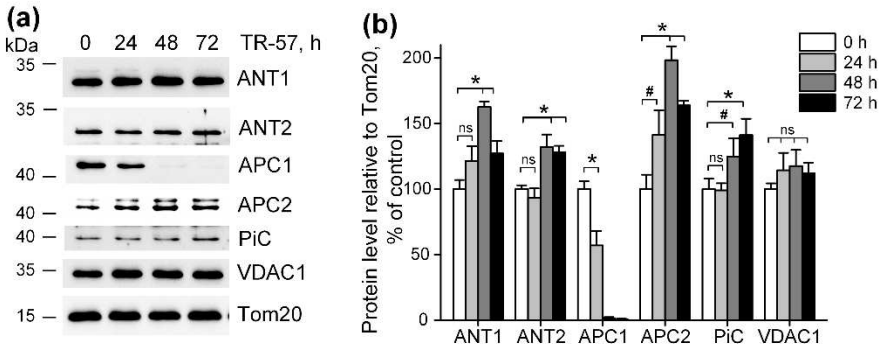

Figure 4. Effect of TR-57 on mitochondrial proteins responsible for ATP and phosphate ion transport. **(a)** Representative Western blots of proteins of control (white bars) SUM159 cells and cells treated with 150 nM TR-57 for 24 h (light gray bars), 48 h (dark gray bars) and 72 h (black bars); **(b)** – quantitative analysis of target protein normalized to Tom20. The ratio of protein level to Tom20 under control conditions was taken as 100%. The data are presented as the means ± SD of at least three independent experiments. The data were analyzed using a one-way ANOVA with post-hoc Bonferroni test. *p > 0.001, "ns" – non significant.

3. Discussion

Mitochondria are key multifunctional intracellular organelles determining the life and death of all cell types through regulation of intracellular supply of ATP, intracellular Ca2+ and redox signaling, metabolic remodeling, apoptotic cell death and intercellular communication [31]. Recent discoveries highlight the role and importance of mitochondria for initiation and development of variety of cancers (for Review See [32]). Oncotic diseases such as leukemia, lymphoma, lung adenocarcinoma, pancreatic ductal adenocarcinoma, as well as cancer stem cells with high metastatic and tumorigenic potential, require large amounts of ATP, fulfilled by upregulation of oxidative phosphorylation [33]. In addition to the production of ATP, mitochondria are involved in the catabolic processes of de novo synthesis of nucleotides, lipids and amino acids necessary for proliferating cells, the formation of ROS signaling molecules, calcium signaling pathway, cell death

 doi:10.20944/preprints202312.0356.v1

regulation [34]. In addition, at present time, targeting specific mitochondrial metabolism gaining attention as an opportunity for development of the efficient cancer cell therapy [34].

Imipridones, a new class of antitumor agents, selectively targeting mitochondria through activating the unique mitochondrial caseinolytic serine protease ClpP [2,9,10]. Mitochondrial effects are associated both directly with the proteolysis of mitochondrial proteins and indirectly through ClpP-dependent activation of the integrated stress response [2,9,13]. It has been demonstrated that majority of mitochondrial processes are disrupted by the action of imipridones, such as imipridone mediated degradation of mtDNA, number of structural and functional proteins of electron-transport chain, tricarboxylic acid cycle, purine and amino acid metabolism, folate-mediated one-carbon metabolism and proline biosynthesis [9,17,30,35].

In our work, we studied the time-dependent effect of TR-57 on the morphological and functional characteristics of mitochondria in triple negative breast cancer cells SUM159. Using SUM159, we demonstrated that TR-57 induces mitochondrial fragmentation, inhibition of the activity of respiratory chain, decline in the number of mtDNA within first 24 hours of exposure of SUM159 cells to 150 nM of TR57. Longer incubation of these cells with TR57 causes neither a further decrease in mitochondrial size nor a change in mitochondrial mass. At the same time, we observed decline in functional state of mitochondria, revealed by inhibition of mitochondrial respiration in a model of digitonin permeabilized cells, oxidizing substrates of ETC Complexes I and II. Manifestation of decrease in the rate of oxygen consumption following TR57 exposure occurs within 24 hours of treatment. Long-term 72-hour incubation with TR-57 leads to complete inhibition of the respiratory chain of mitochondria in SUM159 cells, as we already observed when studying the effect of ONC201 on BT474 cells [21].

A decrease in the activity of respiratory chain complexes can be due to both inhibition of activity and a decrease in the content of complexes. As was previously shown in glioblastoma cells, lymphoblastic leukemia cell line and breast cancer cells, substances of the imipridone group and TR-compounds induce a decrease in the levels of enzymes of Complex I and Complex II of the respiratory chain [9,13–16]. We have shown that during the first 24 hours of treatment of SUM159 cells, the protein content of all four complexes of the mitochondrial respiratory chain drops by more than by 50%, and after 72 hours with the agent, no more than 10% of tested proteins remain. At the same time, the content of F_OF_1-ATPase subunits decreased by 40% on the first day and did not change during further incubation, which correlated with changes in mitochondrial mass. This suggests that TR-57 does not affect the distribution of F_OF_1-ATPase in mitochondria. A finding of great importance is that ATPIF1, the natural mitochondrial ATPase inhibitor protein eliminated early in TR-57 treatment. Previously, proteomic analysis revealed downregulation of IF1 in NALM-6 and SUM 159 cells treated with ONC201 [10,35], which is opposite an increased expression of IF1, observed in various types of carcinomas, and its role in the metabolic shift from oxidative phosphorylation toward glycolysis has been discussed [36]. It has been shown that IF1 promotes proliferation, migration and invasion of tumor cells [36], and selective knockdown of IF1 gene in bladder cancer induced cell proliferation and colony formation [37]. Interestingly, degradation of IF is carried out by an unidentified serine protease [38], and ClpP is precisely this type of protease, allowing one to explain the elimination of IF1 TR-57-induced activation of ClpP and that IF1 could play an important role in the antitumor effect of TR-57.

In our experiments, exposure of SUM159 cells to imipridone TR-57 resulted in complete inhibition of mitochondrial respiration and downregulation of key ETC proteins. However, TR-57 treated cells maintained the mitochondrial membrane potential at a relatively high level. In SUM159 cells treated with TR-57 for 24 hours and less, with partial decline in expression of mitochondrial ETC complex proteins and incomplete inhibition of the mitochondrial respiratory chain activity was sufficient to maintain mitochondrial membrane potential. With long-term treatment with TR-57 and associated inhibition of respiration and substantial decline in the expression of the key component of mitochondrial ETC, mitochondrial membrane potential maintained by the reversed activity of F_OF_1-ATPase, as suggested by dissipation of mitochondrial potential in the presence of oligomycin, a pharmacological inhibitor of ATPase. Post-TR-57 level of the mitochondrial membrane potential was

 doi:10.20944/preprints202312.0356.v1

significantly lower than that maintained by respiration in intact cells, which is in line with the previous observation that the membrane potential, generated by ATP hydrolysis is lower than that supported by respiratory chain alone [39].

We found that exposure of SUM159 cells to TR-57 for up to 72 hours do not change the expression of VDAC1 and ANT1, ANT2, the major proteins, involved in the transport of ATP into the mitochondria of SUM159 cells. ANTs carry out the electrogenic exchange of ATP for ADP across the membrane; the direction of exchange depends on the concentration of a particular nucleotide on different sides of the membrane [40]. It have been demonstrated that ANT2 in tumor cells transports glycolytically synthesized ATP in exchange for ADP into the mitochondrial matrix, and even considered as a marker of proliferation in tumor cells [41]. However, Maldonado et al showed that neither chemical translocase inhibitors nor genetic knockdown of ANT2/3 in tumor cells affected the level of mitochondrial potential maintained by ATP hydrolysis, and concluded that ANT in tumor cells does not participate in transport ATP in mitochondria [42]. Under conditions of low mitochondrial membrane potential, as well as when it is necessary to quickly replenish the ATP content in mitochondria, ATP transport can occur through calcium-regulated mitochondrial ATP-Mg/Pi carriers (SCaMC, APC1/APC2), presenting in cells as 4 paralogues [40]. There are publications that the APC1 isoform is mainly present in tumor cells [43], which is also upregulated in different types of breast cancer cells [44]. However, in our experiments, we observed a decrease in the level of APC1 during short-term treatment of SUM159 cells with TR-57, and an almost complete disappearance of this protein after 48 hours. At the same time, the APC2 isoform increased almost 2-fold at this time point. The content of the inorganic phosphate transporter, which delivers the phosphate necessary for APC function inside the mitochondria, did not change in the presence of TR-57. This allowed us to conclude that the transport of glycolytic ATP into the mitochondrial matrix of TR-57-treated SUM159 cells occurs through APC2. Apparently, despite the fact that the efficiency of ATP transport through APC2 is an order of magnitude lower than through APC1 [45], under the conditions of our work APC2 isoform alone could be sufficient to maintain the membrane potential in mitochondria with an impaired respiratory chain.

The mitochondrial membrane potential provides a number of functions important for cell life: oxidative phosphorylation, calcium transport into mitochondria, transport of metabolites across the inner mitochondrial membrane, import of mitochondrial proteins, regulation of mitophagy and cell death [46]. In tumor cells, mitochondrial potential determines proliferative and metastatic activity and susceptibility to apoptosis [47]. The question of whether mitochondrial potential is involved in maintaining the viability of TR-57-treated SUM159 cells remains the subject of our further research.

In Summary, the effect of the new antitumor agent TR-57 on mitochondrial population in SUM159 cells resulted in fragmentation of mitochondria and essential decrease in the number of mitochondrial nucleoids/mtDNA. Long-term incubation with TR-57 lead to decreased level of Complexes I-IV proteins and to complete suppression of mitochondrial respiration. However, even long-term exposure of SUM159 cells to TR-57 does not lead to complete dissipation of the mitochondrial membrane potential. Our preliminary data demonstrate enhanced sensitivity of mitochondrial membrane potential (evaluated using TMRM) toward oligomycin. We speculate that increased level of ANT-1/2 and APC2 could result in increased transport of cytoplasmic (glycolytic) ATP into the mitochondrial matrix and used by F_OF_1-ATPase in reverse mode to support mitochondrial membrane potential in respiratory chain deficient mitochondria. Understanding the mechanism of action of TR-57 on tumor cells opens up new opportunities for its use in pre-clinical and clinical studies in combination with the inhibitors of mitochondrial respiration and membrane potential and/or glycolysis.

4. Materials and Methods

4.1. Chemicals

TR-57 provided by Madera Therapeutics, LLC (Chapel Hill, NC USA). Hoechst 33342, DiOC6(3) and SYBR Green I were obtained from Invitrogen (Waltham, MA, USA), MitoTracker Deep Red 633

 doi:10.20944/preprints202312.0356.v1

and Tetramethylrhodamine methyl ester (TMRM) were from Molecular Probes (Eugenius, OR, USA), DiOC6(3) was from Sigma-Aldrich (St. Louis, MO, USA). DMEM, HEPES, L-glutamine were obtained from PanEco (Russia). Fetal bovine serum was from Gibco (Carlsbad, CA, USA).

Antibodies to ATPIF1, APC2 (SLC25A23), TFAM, GAPDH, Tom20 were purchased from Santa Cruz (CA, USA), antibodies to subunit β, subunit b, subunit c of mitochondrial ATPase, ANT1, ANT2, APC2 (SLC25A24) and Total OXPHOS antibody cocktail were from Abcam (Cambridge, UK), antibody to TUFM was from Invitrogen (Waltham, MA, USA) and antibody to phosphate carrier (SLC25A23) was from FineTest (Wuhan, China). Secondary goat anti rabbit antibody were purchased from PIERCE (USA) and secondary horse anti mouse antibody was from Cell Signaling (Cell Signaling, Danvers, MA, USA).

Other chemicals used in this work were from Sigma-Aldrich (St. Louis, MO, USA) unless otherwise noted. The concentration of the vehicle (DMSO) used as a solvent for hydrophobic agents was kept under 0.5%.

4.2. Cell culture

Human triple negative breast cancer cells SUM159 were obtained from the ATCC (Manassas, VA, USA). SUM159 cells were cultured in DMEM/F12 medium supplemented with 5% fetal bovine serum, 2.4 g/L $NaHCO_3$, 2 mM L-glutamine, 5 μg/mL insulin, 1 μg/ mL hydrocortisone and a 1% mixture of antibiotic-antimycotic in a cell culture incubator (Binder, USA) set at 37°C in a humidified atmosphere of 5%/CO2. SUM159 cells were seeded and cultured overnight in culture dishes (Corning, NY, USA) at density of 15,000-25,000 cells/sm^2. Following overnight cell adhesion, incubation media in experimental dishes was replaced with the fresh media supplemented with 150 nM TR-57 and cells were treated with drug for 24, 48 and 72 h.

4.3. Analysis of mitochondrial nucleoids, mitochondrial mass and size

For confocal microscopy experiments, SUM159 cells were plated on 35-mm Petri dishes at density 15,000 cells/cm^2, and treated with 150 nM TR-57 for 24, 48 and 72 hours. After treatment, cells were rinsed three times with 2 mL of HBSS and incubated in 2 mL of HBSS, supplemented with 2 μg/mL Hoechst 33342, SYBR Green I at dilution of 1:200000, and 150 nM MitoTracker Deep Red 633 at 37°C for 30 min in CO2-free thermostat. Following staining, the cells were washed 3 times with dye-free HBSS and 3-channel fluorescent images of cells were obtained using laser scanning confocal microscope Leica TCS SP-5 DM6000 CS (Leica Microsystems, Germany), at sequential scanning mode using HCX PL APO lambda blue 63x lens, NA = 1.4, Leica Microsystems, Germany). Excitation and emission were set for Hoechst 33342 405 nm/460 nm, SYBR Green I 488 nm/540 nm, and MitoTracker Deep Red 633 – 633 nm/710 nm. For every sample 5 images from random fields were acquired.

Image analysis was performed using ImageJ software [24]. We analyzed number of mt-nucleoids per cell, average size of mitochondria as described in [25]. Briefly, images were separated into three channels: blue (Hoechst 33342), green (SYBG Green I) and red (MitoTracker Deep Red). A mask was created for each channel: mask of nuclei (blue channel), mask of mitochondrial nucleoids (in green channel) and mask of mitochondria (in red channel). Mask of blue channel was used to quantify number of nuclei on the image, green channel – to quantify number of mitochondrial nucleoids and red channel – to quantify average mitochondrial size. Additionally, we analyzed intensity of MitoTracker Deep Red fluorescence as a parameter of mitochondrial mass. For this purpose, we measured fluorescence intensity of MitoTracker Deep Red within mask of mitochondria and divided on the number of nuclei.

4.4. Mitochondrial respiration in permeabilized SUM159 cells

Harvested control and TR-57-treated cells in the amount of 4×106 cell per probe were washed ones with ice-cold PBS, pelleted at 300g for 2 min and resuspended in 1 ml of respiration medium containing 110 mM KCl, 5 mM NaCl, 5 mM KH_2PO_4, 10 mM HEPES (pH 7.4). Incubation medium was supplemented with 5 mM glutamate + 5 mM malate (Complex I substrate) or 10 mM succinate +

 doi:10.20944/preprints202312.0356.v1

1 μg/mL rotenone (Complex II substrate). Cells transferred into 1 mL of closed measuring chamber of multichannel recorder FluoFlux-Æ1 (Econix-Expert Inc., Moscow, Russian Federation, webpage: http://ionomer.ru) and mitochondrial respiration measured using dissolved oxygen sensor based on the phosphorescence quenching method [48]. After permeabilization of the cellular plasma membrane with 0.003% digitonin and subsequent additions of 2 mM ADP, 5 μM carboxyatractyloside (CATR), 30 μM 2,4-dinitrophenol (DNP) and 1 mM NaN3 as described in [21].

4.5. Measurement of mitochondrial membrane potential and mitochondrial mass using flow cytometry

The intact and TR-57-treated SUM159 cells were washed three times with PBS and detached from the surface of the culture plastic using 0.05% trypsin-EDTA solution. Cell aliquots containing equal cell amount (500 000 cells) were stained for 30 min in a CO2 incubator in the full incubation medium (DMEM/F12) with 10 nM 3,3′-dihexyloxacarbocyanine iodide (DiOC6(3)) to measure mitochondrial membrane potential or with 50 nM MitoTracker Deep Red to assess mitochondrial mass. Experimental data obtained using BD Accuri C6 flow cytometer (BD Bioscience, USA) were processed using BD Accuri C6 CFlow software (BD Bioscience, USA) and resulting histograms were plotted using FlowJo v10 software (BD Bioscience, USA).

4.6. Membrane potential measurement in intact cells using fluorescence microscopy

SUM159 cells were plated on 0.13 mm thick 25-mm round coverslips (Menzel-Gläser, Germany) in 35 mm Petri dishes at a density of 10,000 cells/cm2 and treated with 150 nM TR-57 for 24, 48 and 72 hours. Following TR-57 treatment coverslips with cells were incubated in 1 ml of complete incubation medium containing 20 mM HEPES (PanEco) and 20 nM TMRM for 30 minutes in a cell culture incubator (95/5% air/CO2). After staining, the incubation media was replaced with a similar one containing 20 nM TMRM, and the cells were transferred to a microscopic stage. A Leica DMI6000 B fluorescence microscope (Leica microsystems, Germany) equipped with Hamamatsu EM-CCD digital camera C9100 (Hamamatsu, Japan), the OSRAM HXP R 120W/45C UV mercury lamp, HC PL APO 20x/0.70 water immersion lens, green excitation filter (530 nm), red 640 mm emission filter were used to evaluate TMRM fluorescence. Exposure time was set to 100 ms. 2x2 camera binning, gain 1100, an additional magnification lens 1.6x and 50% neutral density filter were used to decrease excitation light intensity. Time-lapse images were acquired frame by frame with an interval of 1 frame per minute. The baseline (initial TMRM fluorescence) was taken for 5 minutes, then 2 μM oligomycin was added to the cells and the change in TMRM fluorescence was recorded for 5 minutes, after that 5 μM antimycin A and 1 μM CCCP uncoupler were added and the images were acquired for 5 minutes each. Obtained stacks were analyzed using FiJi software as described [24]. The level of mitochondrial membrane potential was determined as intensity of TMRM fluorescence averaged from 5 min of baseline. For tracking of changes in mitochondrial membrane potential in each series, 10 regions of cell mitochondria and 10 corresponding regions of nuclei and 1 region of the extracellular environment were selected, and the fluorescence of TMRM was measured. The relative level of membrane potential ($\Delta\psi$) was calculated using the following formula:

$\Delta\psi = (F_{mt} - F_{background})/(F_{nucleus} - F_{background})$, where F_{mt} is the average fluorescence level of the mitochondrial region of the cell, $F_{nucleus}$ is the average fluorescence level of the cell nucleus area, $F_{background}$ is the average fluorescence level of the extracellular area. Obtained values of membrane potential at each point were normalized to baseline level (referred as 100%) and CCCP (referred as 0%).

4.7. Western blot analysis of mitochondrial proteins

Intact and TR-57-treated cells (4×106) were trypsinized, washed twice in PBS, pelleted at 300×g for 5 min and lysed in RIPA Lysing Buffer System with 1 mM Na_3VO_4, 2 mM PMSF, and a complete protease inhibitor cocktail (Santa Cruz, CA, USA). Samples were solubilized in Laemmli loading buffer (BioRad, Hercules, CA, USA) and boiled at 95°C for 5 min (except samples for Total OXPHOS detection heated at 37°C for 5 min). The concentration of protein in samples was measured by

Bradford method and 30 μg of each sample were subjected to PAAG electrophoresis followed by transfer to nitrocellulose membrane. Then membranes were blocked with 5% dry milk in PBST for 1 h at room temperature and incubated overnight at 4°C with primary antibodies against target proteins. After incubation with corresponding secondary antibodies conjugated with HRP for 1h at room temperature target proteins were visualized with ClarityWestern ECL substrate (Bio-Rad, Hercules, CA, USA). Chemiluminescence was detected with Chemidoc Touch Imaging System (Bio-Rad, Hercules, CA, USA) and Image Lab software was used for the processing and quantification of obtained results.

4.8. Statistical analysis

All experiment performed at least in triplicates were analyzed using the ANOVA one-way variance analysis with a post hoc Bonferroni test [21] and values are presented as mean ± SD and statistical significance of $p<0.05$.

Author Contributions: Conceptualization, E.H. and I.O.; methodology, A.M.,E.M., M.K., E.H.; software, A.M., A.B..; formal analysis, A.M., I.O.; investigation, A.M., E.M., A.V.B., M.K., Y.L., I.O..; resources, A.B., I.O.; writing—original draft preparation, A.M., I.O.; writing—review and editing, A.V.B., E.H., I.O.; visualization, A.M., M.K., Y.L., I.O; supervision, E.H., I.O.; project administration, E.H. and I.O.; funding acquisition, I.O. All authors have read and agreed to the published version of the manuscript.

Funding: This research was funded by Russian Science Foundation, grant number 23-25-00160.

Institutional Review Board Statement: Not applicable.

Informed Consent Statement: Not applicable.

Data Availability Statement: Data are available within the article.

Acknowledgments: We gratefully acknowledge Dr. Lee Graves (University of North Carolina at Chapel Hill, NC USA) for materials and intellectual support and Dr. Mikoulinskaia G.V. (Branch of Shemyakin & Ovchinnikov's Institute of Bioorganic Chemistry RAS., Pushchino, Russian Federation) for the helpful discussion. The study was performed using the equipment at the Center of Collective Use of the Institute of Theoretical and Experimental Biophysics of the Russian Academy of Sciences (http://ckp-rf.ru/ckp/3037/) and the Pushchino Center of Biological Research (http://www.ckp-rf.ru/ckp/670266/).

Conflicts of Interest: The authors declare no conflict of interest. The funders had no role in the design of the study; in the collection, analyses, or interpretation of data; in the writing of the manuscript; or in the decision to publish the results.

References

1. Allen, J.E.; Krigsfeld, G.; Patel, L.; Mayes, P.A.; Dicker, D.T.; Wu, G.S.; El-Deiry, W.S. Identification of TRAIL-inducing compounds highlights small molecule ONC201/TIC10 as a unique anti-cancer agent that activates the TRAIL pathway. Mol Cancer 2015, 14, 99, doi:10.1186/s12943-015-0346-9.
2. Graves, P.R.; Aponte-Collazo, L.J.; Fennell, E.M.J.; Graves, A.C.; Hale, A.E.; Dicheva, N.; Herring, L.E.; Gilbert, T.S.K.; East, M.P.; McDonald, I.M.; et al. Mitochondrial Protease ClpP is a Target for the Anticancer Compounds ONC201 and Related Analogues. ACS Chem Biol 2019, 14, 1020-1029, doi:10.1021/acschembio.9b00222.
3. Allen, J.E.; Krigsfeld, G.; Mayes, P.A.; Patel, L.; Dicker, D.T.; Patel, A.S.; Dolloff, N.G.; Messaris, E.; Scata, K.A.; Wang, W.; et al. Dual inactivation of Akt and ERK by TIC10 signals Foxo3a nuclear translocation, TRAIL gene induction, and potent antitumor effects. Sci Transl Med 2013, 5, 171ra117, doi:10.1126/scitranslmed.3004828.
4. Prabhu, V.V.; Morrow, S.; Rahman Kawakibi, A.; Zhou, L.; Ralff, M.; Ray, J.; Jhaveri, A.; Ferrarini, I.; Lee, Y.; Parker, C.; et al. ONC201 and imipridones: Anti-cancer compounds with clinical efficacy. Neoplasia 2020, 22, 725-744, doi:10.1016/j.neo.2020.09.005.
5. Allen, J.E.; Kline, C.L.; Prabhu, V.V.; Wagner, J.; Ishizawa, J.; Madhukar, N.; Lev, A.; Baumeister, M.; Zhou, L.; Lulla, A.; et al. Discovery and clinical introduction of first-in-class imipridone ONC201. Oncotarget 2016, 7, 74380-74392, doi:10.18632/oncotarget.11814.
6. Wedam, R.; Greer, Y.E.; Wisniewski, D.J.; Weltz, S.; Kundu, M.; Voeller, D.; Lipkowitz, S. Targeting Mitochondria with ClpP Agonists as a Novel Therapeutic Opportunity in Breast Cancer. Cancers (Basel) 2023, 15, doi:10.3390/cancers15071936.

7. Kline, C.L.B.; Ralff, M.D.; Lulla, A.R.; Wagner, J.M.; Abbosh, P.H.; Dicker, D.T.; Allen, J.E.; El-Deiry, W.S. Role of Dopamine Receptors in the Anticancer Activity of ONC201. Neoplasia 2018, 20, 80-91, doi:10.1016/j.neo.2017.10.002.
8. Ralff, M.D.; Jhaveri, A.; Ray, J.E.; Zhou, L.; Lev, A.; Campbell, K.S.; Dicker, D.T.; Ross, E.A.; El-Deiry, W.S. TRAIL receptor agonists convert the response of breast cancer cells to ONC201 from anti-proliferative to apoptotic. Oncotarget 2020, 11, 3753-3769, doi:10.18632/oncotarget.27773.
9. Ishizawa, J.; Zarabi, S.F.; Davis, R.E.; Halgas, O.; Nii, T.; Jitkova, Y.; Zhao, R.; St-Germain, J.; Heese, L.E.; Egan, G.; et al. Mitochondrial ClpP-Mediated Proteolysis Induces Selective Cancer Cell Lethality. Cancer Cell 2019, 35, 721-737 e729, doi:10.1016/j.ccell.2019.03.014.
10. Jacques, S.; van der Sloot, A.M.; C, C.H.; Coulombe-Huntington, J.; Tsao, S.; Tollis, S.; Bertomeu, T.; Culp, E.J.; Pallant, D.; Cook, M.A.; et al. Imipridone Anticancer Compounds Ectopically Activate the ClpP Protease and Represent a New Scaffold for Antibiotic Development. Genetics 2020, 214, 1103-1120, doi:10.1534/genetics.119.302851.
11. Nouri, K.; Feng, Y.; Schimmer, A.D. Mitochondrial ClpP serine protease-biological function and emerging target for cancer therapy. Cell Death Dis 2020, 11, 841, doi:10.1038/s41419-020-03062-z.
12. Mabanglo, M.F.; Bhandari, V.; Houry, W.A. Substrates and interactors of the ClpP protease in the mitochondria. Curr Opin Chem Biol 2022, 66, 102078, doi:10.1016/j.cbpa.2021.07.003.
13. Greer, Y.E.; Porat-Shliom, N.; Nagashima, K.; Stuelten, C.; Crooks, D.; Koparde, V.N.; Gilbert, S.F.; Islam, C.; Ubaldini, A.; Ji, Y.; et al. ONC201 kills breast cancer cells in vitro by targeting mitochondria. Oncotarget 2018, 9, 18454-18479, doi:10.18632/oncotarget.24862.
14. Ishida, C.T.; Zhang, Y.; Bianchetti, E.; Shu, C.; Nguyen, T.T.T.; Kleiner, G.; Sanchez-Quintero, M.J.; Quinzii, C.M.; Westhoff, M.A.; Karpel-Massler, G.; et al. Metabolic Reprogramming by Dual AKT/ERK Inhibition through Imipridones Elicits Unique Vulnerabilities in Glioblastoma. Clin Cancer Res 2018, 24, 5392-5406, doi:10.1158/1078-0432.CCR-18-1040.
15. Przystal, J.M.; Cianciolo Cosentino, C.; Yadavilli, S.; Zhang, J.; Laternser, S.; Bonner, E.R.; Prasad, R.; Dawood, A.A.; Lobeto, N.; Chin Chong, W.; et al. Imipridones affect tumor bioenergetics and promote cell lineage differentiation in diffuse midline gliomas. Neuro Oncol 2022, 24, 1438-1451, doi:10.1093/neuonc/noac041.
16. Fennell, E.M.J.; Aponte-Collazo, L.J.; Wynn, J.D.; Drizyte-Miller, K.; Leung, E.; Greer, Y.E.; Graves, P.R.; Iwanowicz, A.A.; Ashamalla, H.; Holmuhamedov, E.; et al. Characterization of TR-107, a novel chemical activator of the human mitochondrial protease ClpP. Pharmacol Res Perspect 2022, 10, e00993, doi:10.1002/prp2.993.
17. Greer, Y.E.; Hernandez, L.; Fennell, E.M.J.; Kundu, M.; Voeller, D.; Chari, R.; Gilbert, S.F.; Gilbert, T.S.K.; Ratnayake, S.; Tang, B.; et al. Mitochondrial Matrix Protease ClpP Agonists Inhibit Cancer Stem Cell Function in Breast Cancer Cells by Disrupting Mitochondrial Homeostasis. Cancer Res Commun 2022, 2, 1144-1161, doi:10.1158/2767-9764.CRC-22-0142.
18. Amoroso, F.; Glass, K.; Singh, R.; Liberal, F.; Steele, R.E.; Maguire, S.; Tarapore, R.; Allen, J.E.; Van Schaeybroeck, S.; Butterworth, K.T.; et al. Modulating the unfolded protein response with ONC201 to impact on radiation response in prostate cancer cells. Sci Rep 2021, 11, 4252, doi:10.1038/s41598-021-83215-y.
19. Ishizawa, J.; Kojima, K.; Chachad, D.; Ruvolo, P.; Ruvolo, V.; Jacamo, R.O.; Borthakur, G.; Mu, H.; Zeng, Z.; Tabe, Y.; et al. ATF4 induction through an atypical integrated stress response to ONC201 triggers p53-independent apoptosis in hematological malignancies. Sci Signal 2016, 9, ra17, doi:10.1126/scisignal.aac4380.
20. Kline, C.L.; Van den Heuvel, A.P.; Allen, J.E.; Prabhu, V.V.; Dicker, D.T.; El-Deiry, W.S. ONC201 kills solid tumor cells by triggering an integrated stress response dependent on ATF4 activation by specific eIF2alpha kinases. Sci Signal 2016, 9, ra18, doi:10.1126/scisignal.aac4374.
21. Mishukov, A.; Odinokova, I.; Mndlyan, E.; Kobyakova, M.; Abdullaev, S.; Zhalimov, V.; Glukhova, X.; Galat, V.; Galat, Y.; Senotov, A.; et al. ONC201-Induced Mitochondrial Dysfunction, Senescence-like Phenotype, and Sensitization of Cultured BT474 Human Breast Cancer Cells to TRAIL. Int J Mol Sci 2022, 23, doi:10.3390/ijms232415551.
22. Ralff, M.D.; Kline, C.L.B.; Kucukkase, O.C.; Wagner, J.; Lim, B.; Dicker, D.T.; Prabhu, V.V.; Oster, W.; El-Deiry, W.S. ONC201 Demonstrates Antitumor Effects in Both Triple-Negative and Non-Triple-Negative Breast Cancers through TRAIL-Dependent and TRAIL-Independent Mechanisms. Mol Cancer Ther 2017, 16, 1290-1298, doi:10.1158/1535-7163.MCT-17-0121.
23. Aponte-Collazo, L.J., Fennell, M.J.; East, M.P., Gilbert, T.S.K.; Graves, P.R., Ashamalla, H.; Iwanowicz, E.J.; Greer, Y.E.; Lipkowitz, S.; Graves, L.M. Small molecule ClpP agonists induce senescence and alter TRAIL-mediated apoptotic response of triple-negative breast cancer cells. bioRxiv 2022, doi:10.1101/2022.07.11.499620.

24. Schindelin, J.; Arganda-Carreras, I.; Frise, E.; Kaynig, V.; Longair, M.; Pietzsch, T.; Preibisch, S.; Rueden, C.; Saalfeld, S.; Schmid, B.; et al. Fiji: an open-source platform for biological-image analysis. Nat Methods 2012, 9, 676-682, doi:10.1038/nmeth.2019.
25. Mishukov, A.A.; Berezhnov, A.V.; Kobyakova, M.I.; Evstratova, Y.V.; Mndlyan, E.Y.; Holmuhamedov, E.L. Effect of ONC201 Antitumor Drug on the Number of Mitochondrial Nucleoids in BT474 Breast Cancer Cells in Culture. Moscow University Biological Sciences Bulletin 2021, 76, 83-89, doi:10.3103/S0096392521030111.
26. Nicholls, D.G. The influence of respiration and ATP hydrolysis on the proton-electrochemical gradient across the inner membrane of rat-liver mitochondria as determined by ion distribution. Eur J Biochem 1974, 50, 305-315, doi:10.1111/j.1432-1033.1974.tb03899.x.
27. Ezaki, J.; Wolfe, L.S.; Kominami, E. Specific delay in the degradation of mitochondrial ATP synthase subunit c in late infantile neuronal ceroid lipofuscinosis is derived from cellular proteolytic dysfunction rather than structural alteration of subunit c. J Neurochem 1996, 67, 1677-1687, doi:10.1046/j.1471-4159.1996.67041677.x.
28. Li, H.S.; Zhang, J.Y.; Thompson, B.S.; Deng, X.Y.; Ford, M.E.; Wood, P.G.; Stolz, D.B.; Eagon, P.K.; Whitcomb, D.C. Rat mitochondrial ATP synthase ATP5G3: cloning and upregulation in pancreas after chronic ethanol feeding. Physiol Genomics 2001, 6, 91-98, doi:10.1152/physiolgenomics.2001.6.2.91.
29. Geiss, C.; Witzler, C.; Poschet, G.; Ruf, W.; Regnier-Vigouroux, A. Metabolic and inflammatory reprogramming of macrophages by ONC201 translates in a pro-inflammatory environment even in presence of glioblastoma cells. Eur J Immunol 2021, 51, 1246-1261, doi:10.1002/eji.202048957.
30. Pruss, M.; Dwucet, A.; Tanriover, M.; Hlavac, M.; Kast, R.E.; Debatin, K.M.; Wirtz, C.R.; Halatsch, M.E.; Siegelin, M.D.; Westhoff, M.A.; et al. Dual metabolic reprogramming by ONC201/TIC10 and 2-Deoxyglucose induces energy depletion and synergistic anti-cancer activity in glioblastoma. Br J Cancer 2020, 122, 1146-1157, doi:10.1038/s41416-020-0759-0.
31. Bock, F.J.; Tait, S.W.G. Mitochondria as multifaceted regulators of cell death. Nat Rev Mol Cell Biol 2020, 21, 85-100, doi:10.1038/s41580-019-0173-8.
32. Martinez-Reyes, I.; Chandel, N.S. Cancer metabolism: looking forward. Nat Rev Cancer 2021, 21, 669-680, doi:10.1038/s41568-021-00378-6.
33. Ashton, T.M.; McKenna, W.G.; Kunz-Schughart, L.A.; Higgins, G.S. Oxidative Phosphorylation as an Emerging Target in Cancer Therapy. Clin Cancer Res 2018, 24, 2482-2490, doi:10.1158/1078-0432.CCR-17-3070.
34. Weinberg, S.E.; Chandel, N.S. Targeting mitochondria metabolism for cancer therapy. Nat Chem Biol 2015, 11, 9-15, doi:10.1038/nchembio.1712.
35. Fennell, E.M.J.; Aponte-Collazo, L.J.; Pathmasiri, W.; Rushing, B.R.; Barker, N.K.; Partridge, M.C.; Li, Y.Y.; White, C.A.; Greer, Y.E.; Herring, L.E.; et al. Multi-omics analyses reveal ClpP activators disrupt essential mitochondrial pathways in triple-negative breast cancer. Front Pharmacol 2023, 14, 1136317, doi:10.3389/fphar.2023.1136317.
36. Gore, E.; Duparc, T.; Genoux, A.; Perret, B.; Najib, S.; Martinez, L.O. The Multifaceted ATPase Inhibitory Factor 1 (IF1) in Energy Metabolism Reprogramming and Mitochondrial Dysfunction: A New Player in Age-Associated Disorders? Antioxid Redox Signal 2022, 37, 370-393, doi:10.1089/ars.2021.0137.
37. Wei, S.; Fukuhara, H.; Kawada, C.; Kurabayashi, A.; Furihata, M.; Ogura, S.; Inoue, K.; Shuin, T. Silencing of ATPase Inhibitory Factor 1 Inhibits Cell Growth via Cell Cycle Arrest in Bladder Cancer. Pathobiology 2015, 82, 224-232, doi:10.1159/000439027.
38. Sanchez-Arago, M.; Garcia-Bermudez, J.; Martinez-Reyes, I.; Santacatterina, F.; Cuezva, J.M. Degradation of IF1 controls energy metabolism during osteogenic differentiation of stem cells. EMBO Rep 2013, 14, 638-644, doi:10.1038/embor.2013.72.
39. Chinopoulos, C. Mitochondrial consumption of cytosolic ATP: not so fast. FEBS Lett 2011, 585, 1255-1259, doi:10.1016/j.febslet.2011.04.004.
40. Lytovchenko, O.; Kunji, E.R.S. Expression and putative role of mitochondrial transport proteins in cancer. Biochim Biophys Acta Bioenerg 2017, 1858, 641-654, doi:10.1016/j.bbabio.2017.03.006.
41. Chevrollier, A.; Loiseau, D.; Chabi, B.; Renier, G.; Douay, O.; Malthiery, Y.; Stepien, G. ANT2 isoform required for cancer cell glycolysis. J Bioenerg Biomembr 2005, 37, 307-316, doi:10.1007/s10863-005-8642-5.
42. Maldonado, E.N.; DeHart, D.N.; Patnaik, J.; Klatt, S.C.; Gooz, M.B.; Lemasters, J.J. ATP/ADP Turnover and Import of Glycolytic ATP into Mitochondria in Cancer Cells Is Independent of the Adenine Nucleotide Translocator. J Biol Chem 2016, 291, 19642-19650, doi:10.1074/jbc.M116.734814.
43. Traba, J.; Del Arco, A.; Duchen, M.R.; Szabadkai, G.; Satrustegui, J. SCaMC-1 promotes cancer cell survival by desensitizing mitochondrial permeability transition via ATP/ADP-mediated matrix Ca(2+) buffering. Cell Death Differ 2012, 19, 650-660, doi:10.1038/cdd.2011.139.
44. Chen, Y.W.; Chou, H.C.; Lyu, P.C.; Yin, H.S.; Huang, F.L.; Chang, W.S.; Fan, C.Y.; Tu, I.F.; Lai, T.C.; Lin, S.T.; et al. Mitochondrial proteomics analysis of tumorigenic and metastatic breast cancer markers. Funct Integr Genomics 2011, 11, 225-239, doi:10.1007/s10142-011-0210-y.

45. Fiermonte, G.; De Leonardis, F.; Todisco, S.; Palmieri, L.; Lasorsa, F.M.; Palmieri, F. Identification of the mitochondrial ATP-Mg/Pi transporter. Bacterial expression, reconstitution, functional characterization, and tissue distribution. J Biol Chem 2004, 279, 30722-30730, doi:10.1074/jbc.M400445200.
46. Zorova, L.D.; Popkov, V.A.; Plotnikov, E.Y.; Silachev, D.N.; Pevzner, I.B.; Jankauskas, S.S.; Babenko, V.A.; Zorov, S.D.; Balakireva, A.V.; Juhaszova, M.; et al. Mitochondrial membrane potential. Anal Biochem 2018, 552, 50-59, doi:10.1016/j.ab.2017.07.009.
47. Begum, H.M.; Shen, K. Intracellular and microenvironmental regulation of mitochondrial membrane potential in cancer cells. WIREs Mech Dis 2023, 15, e1595, doi:10.1002/wsbm.1595.
48. Zaitsev, N.K., Melnikov, P. V., Alferov, V. A., Kopytin, A. V., German, K. E. . Stable Optical Oxygen Sensing Material Based on Perfluorinated Polymer and Fluorinated Platinum(II) and Palladium(II) Porphyrins. Procedia Engineering 2016, 168, 309-312, doi:10.1016/j.proeng.2016.11.203.